

Buckling loads of columns of regular polygon cross-section with constant volume and clamped ends

Byoung Koo Lee

Dept. of Civil Engineering, Wonkwang University, Iksan, Junbuk, 570-749, Korea

Email: bkleest@wonkwang.ac.kr

Sang Jin Oh

Dept. of Civil Engineering, Provincial College of Damyang, Damyang, Chonnam, 517-800, Korea

Email: sjoh@damyang.damyang.ac.kr

Guangfan Li

Dept. of Civil Engineering, Yanbian University, Yanji 13300, China

ABSTRACT

A numerical method is developed for calculating the buckling loads of tapered columns of regular polygon cross-section with constant volume and both clamped ends. The linear, parabolic and sinusoidal tapers are considered in numerical examples. From the numerical results, the strongest columns by the taper types and side numbers of regular polygon cross-sections are identified.

KEYWORDS

Buckling load; constant volume; strongest column; tapered column

1. Introduction

Since columns are basic structural forms, these units have been widely used in various engineering fields. Estimating the buckling loads of non-prismatic columns, which have the same volume with specific span length, are attractive in the viewpoint of optimal design. Since Lagrange [1] had attempted to determine the optimum shape for a column, many investigators including Keller [2], Tadjbakhsh and Keller [3], Barnes [4] and Cox and Overton [5] determined the shape of the strongest column. In this study, the strongest column is defined as the elastic column of given both length and volume, which can carry the highest axial load without buckling. Lee and Oh [6] calculated the buckling loads of columns of constant volume.

Nowhere in the open literature, the solutions for the class of buckling problems considered herein: buckling loads of non-uniform or tapered columns of regular polygon cross-section with constant volume and both clamped ends, whose cross-sectional depths are varied by functional fashions are given. The purpose of this paper is to investigate the buckling loads of such columns and the configurations of strongest columns.

2. Object column

Shown in Figure 1(a) is the object column of specific span length l and of constant volume V , which is supported by both clamped ends. All the columns analyzed in this study have the same span length and same volume. Its cross-sectional shape is the regular polygon whose cross-sectional depth depicted as h varies with the axial length s . The area and area moment of inertia of cross section depicted as A and I , respectively, vary with s . Figure 1(b) shows the

variation of depth h with s . As shown in this figure, the depth h is varied by functional fashion, and depths h at $s=0$ and l , and at $s=l/2$ are h_0 and h_m , respectively. For defining the geometry of column, a non-dimensional system parameter or section ratio n is introduced as follows.

$$n = h_m / h_0 \tag{1}$$

The quantities A and I of the regular polygon cross-section with integer m of side number and cross-sectional depth h are expressed in the forms

$$A = c_1 h^2, \tag{2}$$

$$I = c_2 h^4, \tag{3}$$

where

$$c_1 = m \sin(\pi/m) \cos(\pi/m), \tag{4.1}$$

$$c_2 = m \sin(\pi/m) \cos^3(\pi/m) [1 + \tan^2(\pi/m) / 3] / 4. \tag{4.2}$$

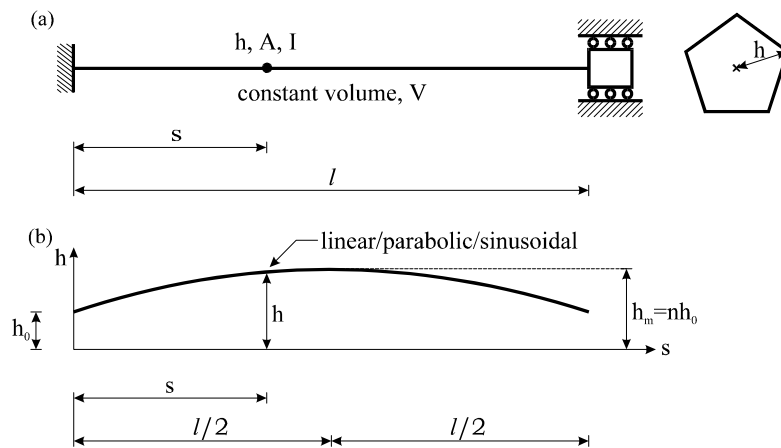


Figure 1 - (a) Column of regular polygon cross-section with constant volume and (b) Its variation of cross-sectional depth.

Now, consider the functional equations of variable depth h . It is natural that all columns whose variable depths are prescribed should be the object ones. In this study, the linear, parabolic and sinusoidal tapers are chosen for the variable depth h of tapered column. First, the equation h of linear taper through three points of $(0, h_0)$, $(l/2, nh_0)$ and (l, h_0) in rectangular co-ordinates (s, h) is obtained. The result is

$$\left. \begin{aligned} h &= h_0 [2c_3 (s/l) + 1], & 0 \leq s \leq l/2, \\ h &= h_0 [-2c_3 (s/l) + 2c_3 + 1], & l/2 \leq s \leq l, \end{aligned} \right\} \tag{5}$$

Where

$$c_3 = n - 1. \tag{6}$$

The column's volume V can now be calculated by using equations (2) and (5):

$$V = \int_0^l A ds = c_4 (c_1 h_0^2 l), \tag{7}$$

where

$$c_4 = V / (c_1 h_0^2 l) = (n^2 + n + 1) / 3. \tag{8}$$

In above equation (8), the coefficient c_4 is defined as a ratio of constant volume V to volume of uniform column of regular polygon cross-section with depth h_0 , $c_1 h_0^2 l$.

Second, the equation h and coefficient c_4 of parabolic taper are, respectively,

$$h = h_0 [-4c_3 (s/l)^2 + 4c_3 (s/l) + 1], \quad 0 \leq s \leq l, \tag{9}$$

$$c_4 = (8n^2 + 4n + 3) / 15. \tag{10}$$

Finally, the equation h and coefficient c_4 of sinusoidal taper are, respectively,

$$h = h_0 [c_3 \sin(\pi s / l) + 1], \quad 0 \leq s \leq l, \tag{11}$$

$$c_4 = (n - 1)^2 / 2 + 4(n - 1) / \pi + 1. \tag{12}$$

In equations (9) and (11), the coefficient c_3 is defined in previous equation (6).

3. Mathematical model

The object column is subjected to a compressive load P as shown in Figure 2. The column subjected to a load P less than the buckling load B is perfectly straight. But when the P exceeds the B , the column is buckled. The dashed line and solid curve are the neutral axes of the unbuckled and buckled columns, respectively. Thus the shape of elastica is the solid curve defined by the (x, y) co-ordinate system whose origin is at left end. At material point (x, y) , the column's arc length is s , and the variable area moment of inertia of cross section taken with respect to s is I discussed in above section. Also the rotation of cross-section and bending moment are depicted as θ and M , respectively. It is noted that the axis length of buckled column maintains its length l due to incompressibility of column, and therefore the value s at right end is l . The end moments at both ends ($s=0$ and $s=l$) are M_0 . It is assumed that Bernoulli-Euler theory governs the buckled column behavior under load, for which the differential equations for the elastica are

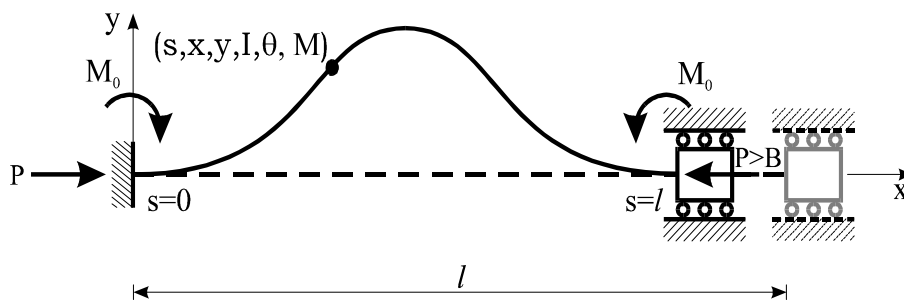


Figure 2 - Variables of elastica of buckled column.

$$d\theta / ds = (M_0 - Py) / EI, \quad 0 \leq s \leq l, \tag{13}$$

$$dx / ds = \cos \theta, \quad 0 \leq s \leq l, \tag{14}$$

$$dy/ds = \sin \theta, \quad 0 \leq s \leq l, \quad (15)$$

where E is Young's modulus and the term of $(M_0 - Py)$ in equation (13) is the bending moment M at the material point (x, y) .

Since the horizontal and vertical displacements and rotation at left end ($s=0$) are not allowed, the following boundary conditions are obtained:

$$x = 0 \text{ at } s = 0, \quad (16)$$

$$y = 0 \text{ at } s = 0, \quad (17)$$

$$\theta = 0 \text{ at } s = 0. \quad (18)$$

Since the rotation at mid-point of buckled column axis ($s=l/2$) is zero due to the symmetry of column geometry, the boundary condition is

$$\theta = 0 \text{ at } s = l/2. \quad (19)$$

When the differential equations (13) - (15) with the boundary conditions of equations (16) - (19) are solved by the appropriate numerical methods, the non-linear behaviors of buckled columns such as the elastica and equilibrium path are obtained. However, such problem is beyond the purpose of this study.

To facilitate the numerical studies and to obtain the most general results for this class of problem, the axial load, the end moment, the co-ordinates, and the governing differential equations with their boundary conditions are cast in the following non-dimensional forms.

The load parameters p and m_0 are defined as

$$p = Pl^2 / (\pi^2 EI_c), \quad (20)$$

$$m_0 = M_0 l / (\pi^2 EI_c), \quad (21)$$

where I_c is the area moment of inertia of circular cross-section of uniform column whose volume is V , defined as

$$I_c = V^2 / (4\pi l^2). \quad (22)$$

Note that the load parameters p and m_0 of equations (20) and (21) with equation (22) are defined by using the constant volume V and the column length l in order to compare all the responses of columns regardless of taper type, side number m and section ratio n .

The arc length s and coordinates (x, y) are normalized by the column length l :

$$\lambda = s/l, \quad (23)$$

$$\xi = x/l, \quad (24)$$

$$\eta = y/l. \quad (25)$$

When equation (3) is combined with either equation (5) or equation (9) or equation (11), and equations (20)-(25) are used, the non-dimensional form of equation (13) becomes

$$d\theta/d\lambda = \pi c_1^2 c_4^2 (m_0 - p\eta)/(4c_2 i), \quad 0 \leq \lambda \leq 1, \quad (26.1)$$

where

$$\text{for linear taper : } \left. \begin{aligned} i &= (2c_3\lambda + 1)^4, \quad 0 \leq \lambda \leq 0.5, \\ i &= (-2c_3\lambda + 2c_3 + 1)^4, \quad 0.5 \leq \lambda \leq 1, \end{aligned} \right\} \quad (26.2)$$

$$\text{for parabolic taper : } i = (-4c_3\lambda^2 + 4c_3\lambda + 1)^4, \quad 0 \leq \lambda \leq 1, \quad (26.3)$$

$$\text{for sinusoidal taper : } i = [c_3 \sin(\pi\lambda) + 1]^4, \quad 0 \leq \lambda \leq 1. \quad (26.4)$$

It is recalled that the coefficients c_1 - c_4 of differential equation (26.1) with equations (26.2)-(26.4) contain the side number m and section ratio n , respectively, as shown in the previous section.

Just after the column is buckled, all values of column behavior including m_0 are closed to zero. In this study, the buckling load parameter b is approximately equivalent to the load parameter p whose end moment m_0 is 1×10^{-10} , i.e. nearly zero but not zero. Substituting $m_0 = 1 \times 10^{-10}$ and $p = b$ into equation (26.1) gives

$$d\theta/d\lambda = \pi c_1^2 c_4^2 (1 \times 10^{-10} - b\eta)/(4c_2 i), \quad 0 \leq \lambda \leq 1 \quad (27.1)$$

in which the buckling load parameter b is defined as

$$b = Bl^2/(\pi^2 EI_c). \quad (27.2)$$

Further, with equations (23)-(25), equations (14) and (15) become

$$d\xi/d\lambda = \cos \theta, \quad 0 \leq \lambda \leq 1, \quad (28)$$

$$d\eta/d\lambda = \sin \theta, \quad 0 \leq \lambda \leq 1. \quad (29)$$

The non-dimensional forms for boundary conditions of equations (16)-(19) are obtained by equations (23)-(25):

$$\xi = 0 \text{ at } \lambda = 0, \quad (30)$$

$$\eta = 0 \text{ at } \lambda = 0, \quad (31)$$

$$\theta = 0 \text{ at } \lambda = 0, \quad (32)$$

$$\theta = 0 \text{ at } \lambda = 1/2. \quad (33)$$

4. Numerical methods

Based on above analysis, the algorithm was developed to solve differential equations (27.1), (28) and (29) for calculating the buckling load parameter b . The Runge-Kutta and Regula-Falsi methods were used to integrate differential equations and to determine the b for a given geometry of column. This algorithm is summarized as follows.

- (1) Specify taper type (linear/parabolic/sinusoidal) and geometry (m and n), and calculate c_1 - c_4 .
- (2) Assume a trial value b in which the first trial value is 0.
- (3) Integrate equations (27.1), (28) and (29) with the boundary conditions of equations (30)-

(32) in the range from $\lambda=0$ to $1/2$ using the Runge-Kutta method. The results give trial solutions for $\theta=\theta(\lambda)$, $\xi=\xi(\lambda)$ and $\eta=\eta(\lambda)$.

- (4) Set $D=\theta(1/2)$. If the value of b assumed in step 2 is the characteristic value of the elastica, then D must be zero due to equation (33). The first criterion for convergence of the solutions is $|D|\leq 1\times 10^{-10}$.
- (5) If the value of D does not satisfy the first convergence criterion, then increment the previous trial value b .
- (6) Repeat steps (3)-(5) and note the sign of D in each iteration. If D changes sign between two consecutive trial values b_1 and b_2 , then the characteristic value b lies between b_1 and b_2 .
- (7) Compute an improved value b_3 based on its two previous values b_1 and b_2 using the Regula-Falsi method. The second criterion for convergence of solutions is $|(b_2-b_1)/b_2|\leq 1\times 10^{-5}$ for which $D_1\times D_2 < 0$ in which D_1 and D_2 are the D values corresponding b_1 and b_2 , respectively.
- (8) Terminate the calculations when two convergence criteria are met. Print the b_2 as the approximate buckling load parameter b .

Based on this algorithm, a FORTRAN computer program was written to solve the buckling load. All computations were carried on a notebook computer with graphics support. For all of the numerical results presented herein, a step size of $\Delta\lambda=(1/2)/50$ in the Runge-Kutta method was found to give convergence for b to within three significant figures.

5. Numerical results and discussions

For the purpose of validation of this study, the buckling load parameters b predicted by the present theory are compared to those available in references [7,8] in Table 1. This table shows the results of this study agree quite well with the reference values, in which ‘ $m=c$ ’ in geometry column means the circular cross-section, namely $m=\infty$.

Table 1 - Comparisons of b between this study and references

Geometry	Buckling load parameter, b	
	This study	Reference
$n=1. *, m=c$	$b=4.0$	4.0 of Ref. [7]
$n = 0.836, m = 3$	$b = 4.929$	} of Ref.[8]
$n = 0.836, m = 4$	$b = 4.269$	
$n = 0.836, m = 5$	$b = 4.145$	
$n = 0.836, m = c$ parabolic	$b = 4.076$	

*If $n=1$. the columns are uniform regardless of taper types. See equations (26.2)-(26.4).

Shown in Figures 3-5 are the b versus n curves of columns with $m=3, 4, 5$ and c for linear, parabolic and sinusoidal taper, respectively. Each curve reaches a peak, which is marked by \square . At these peak points, the columns corresponding to the given taper types have the largest b values, which are the buckling load parameters of strongest columns. Here the word ‘strongest’

is used to mean ‘most’ resistant to buckle. It is found that all strongest columns occur at the same value n regardless of side number m if the taper type is same. And all b values of strongest columns decrease, as the value m is increased from 3 to 4 to 5 to c . The values of b and n of all strongest columns are summarized in table 2. From this table, it is noted that all b values of strongest columns are largest at $m=3$ (triangular cross-section) and smallest at $m=c$ (circular cross-section), and the ratios of b of $m=3$ to b of $m=c$ are same, i.e. 1.210, regardless of taper types. Also, this holds true that each ratio of b of $m=4$ and 5 to b of $m=c$ is same regardless of taper types.

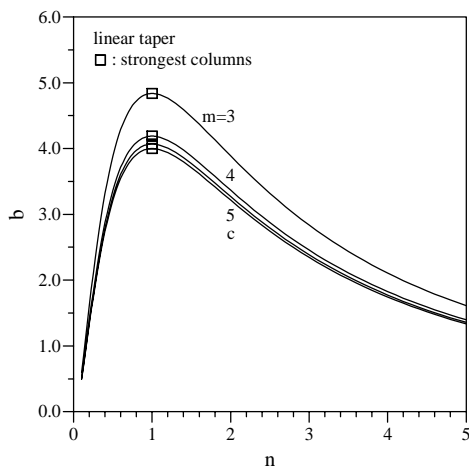


Figure 3 - b vs. n curves of linear taper by side number m .

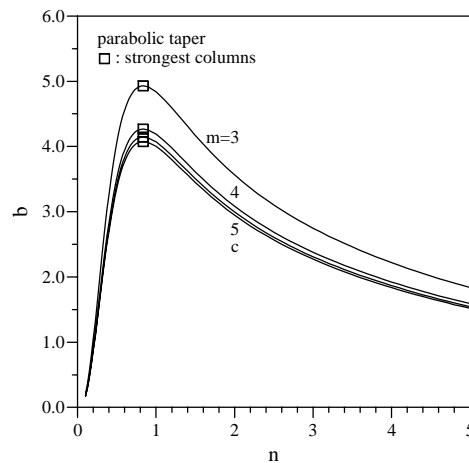


Figure 4 - b vs. n curves of parabolic taper by side number m .

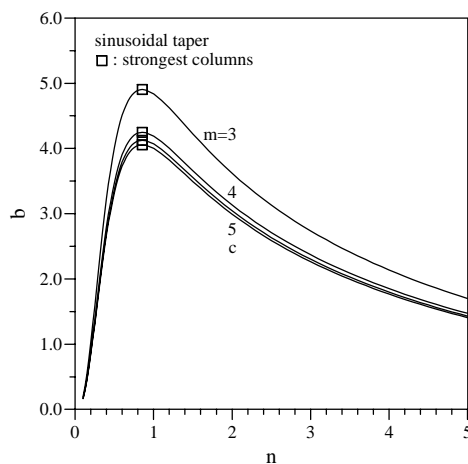


Figure 5 - b vs. n curves of sinusoidal taper by side number m .

Shown in Figure 6 are the b versus n curves of parabolic, sinusoidal and linear tapers, respectively, for $m=3$, in which the strongest columns are marked by \square . It is clear that the strongest of all columns by taper type is the parabolic tapered column as shown in this figure and Table 2. The effect of taper type on b is negligible when n is less than about 0.4.

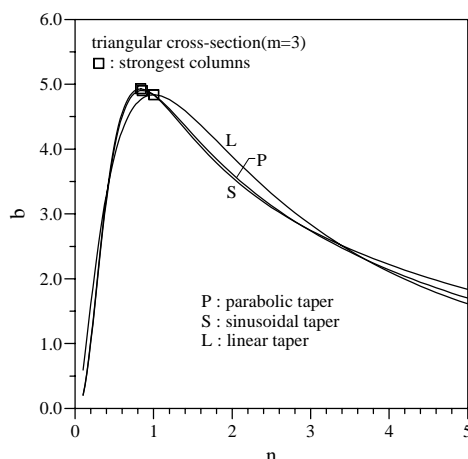


Figure 6 - b vs. n curves by taper type.

Table 2 - Values of n and b of strongest columns by taper type and side number m

Taper type	m	n	b	Ratio*
Linear taper	3	1.00	4.837	1.210
	4	1.00	4.189	1.047
	5	1.00	4.068	1.017
	c	1.00	4.000	1.000
Parabolic taper	3	0.836	4.929	1.210
	4	0.836	4.269	1.047
	5	0.836	4.145	1.017
	c	0.836	4.076	1.000
Sinusoidal taper	3	0.855	4.904	1.210
	4	0.855	4.247	1.047
	5	0.855	4.124	1.017
	c	0.855	4.056	1.000

* Ratio of b of m=3, 4 and 5, respectively, to b of m=c.

6. Concluding remarks

A novel numerical method developed herein for computing the buckling load of tapered column of regular polygon cross-section with constant volume and both clamped ends was found to be efficient, and highly versatile. The linear, parabolic and sinusoidal tapers were chosen for the variable cross-sectional depth. As the numerical results, the buckling load parameters versus section ratio (b vs. n) curves were reported. The strongest columns by taper types and side numbers of regular polygon cross-section were identified by reading the peak points of buckling load parameters and their corresponding section ratios on b versus n curves.

ACKNOWLEDGEMENT

This work was supported by Wonkwang University in 2001. The first author acknowledges this financial support.

REFERENCES

1. Todhunter, I. and Pearson, K., A History of the Theory of Elasticity and of the Strength of Materials, Cambridge Press, 1886.
2. Keller, J. B., "The shape of the strongest column," *Archive for Rational Mechanics and Analysis*, Vol. 5, 1960, pp. 275-285.
3. Tadjbakhsh, I. and Keller, J. B., "Strongest columns and isoperimetric inequalities for eigenvalues," *Journal of Applied mechanics, ASME*, Vol. 29, 1962, pp. 159-164.
4. Barnes, D. C., "The shape of the strongest column is arbitrarily close to the shape of the weakest column," *Quarterly of Applied Mathematics*, Vol. 46, 1988, pp. 605-609.
5. Cox, S. J. and Overton, M. I., "On the optimal design of columns against Buckling," *SIAM Journal on Mathematical Analysis*, Vol. 23, 1992, pp. 287-325.
6. Lee, B.K. and S.J. Oh, "Elastica and buckling load of simple tapered column with constant volume," *International Journal of Solids and Structures*, Vol. 37, No. 18 2000, pp. 2507-2518.
7. Timoshenko, S.P. and Gere, J. M., Theory of Elastic Stability, McGraw-Hill, 1961.
8. Lee, B. K. and Mo, J. M., "Free vibrations and buckling loads of tapered beam-columns of regular polygon cross-section with constant volume," *Journal of Korean Society of Noise and Vibration Engineering*, Vol. 6, No. 5, 1996, pp. 587-594.